Synthesis and Characterization of a Copper-substituted Manganese Oxide with the $Na_{0.44}MnO_2$ Structure

Marca M. Doeff,[a] Thomas J. Richardson,[b] Joel Hollingsworth,[a] Chun-Wei Yuan[a] and Marcela Gonzales[a]

[a] *Materials Sciences Division*

[b] *Environmental Energy Technologies Division*

Lawrence Berkeley National Laboratory

Berkeley, CA 94720

Abstract

$Na_xCu_{0.11}Mn_{0.89}O_2$ (x = 0.4-0.5) with the $Na_{0.44}MnO_2$ structure was prepared by sol-gel, glycine-nitrate combustion synthesis and solid-state routes. $Li_{0.45-x}Cu_{0.11}Mn_{0.89}O_2$ was prepared by ion exchange from the glycine nitrate sodium-containing precursor. Rietveld refinement of x-ray diffraction power patterns indicates that Cu substitutes in the Mn3 position. The electrochemical characteristics of $Li_xCu_{0.11}Mn_{0.89}O_2$ are changed by Cu-substitution, resulting in a somewhat lower capacity between fixed voltage limits compared to the unsubstituted material.

Electrode materials with the $Na_{0.44}MnO_2$ structure (Figure 1) show excellent reversibility towards alkali metal insertion processes.[1] Prior to use in lithium cells, $Na_{0.44}MnO_2$ may be ion-exchanged to yield an isostructural Li_xMnO_2 compound, which does not undergo conversion to spinel during normal cycling, or upon heating below about 400 °C.[2] Little to no capacity fading is seen upon prolonged cycling in either Li/liquid electrolyte cell configurations at room temperature or Li/polymer electrolyte cell configurations at 85 °C.[3] Liquid electrolyte cells containing Li_xMnO_2 discharged repeatedly at up to 5C rate deliver 80% or more of the expected capacity, and cycle normally thereafter, with no signs of damage. The characteristics of stability, robustness, and excellent reversibility make this an attractive material for use in hybrid electric vehicle (HEV) batteries, which must be able to undergo thousands of high power discharges.

At present, factors affecting the electrochemistry of compounds with the $Na_{0.44}MnO_2$ structure are not well understood. Incompletely exchanged materials (i.e. $Li_xNa_yMnO_2$; $x + y \approx 0.44$) and those in which the Mn has been partly substituted by titanium[4] exhibit somewhat different discharge and cycling characteristics than those of Li_xMnO_2. The current work extends the investigation of the effect of metal substitution on the chemistry and electrochemistry of tunnel-containing manganese oxides.

Experimental

Three different routes were used to prepare the sodium-containing precursors: a glycine-nitrate combustion process (GNP)[5], sol-gel synthesis, and solid-state synthesis. For glycine-nitrate combustion, several solutions containing $NaNO_3$, $Cu(NO_3)_2 \cdot 2.5H_2O$,

$Mn(NO_3)_2$ and glycine in water were prepared. The Cu:Mn molar ratio of 0.11:0.89 was fixed and the $NaNO_3$ and glycine content were varied. The solutions were dripped into a heated stainless steel beaker and allowed to combust. The resultant black powders were then calcined at 800 °C for four hours. For the sol-gel preparations, aqueous solutions containing sodium acetate, manganese acetate and $Cu(NO_3)_2 \cdot 2.5H_2O$ were added drop-wise to stirred aqueous glycolic acid solutions (molar ratio of glycolic acid to total metal ions was 1:1). Again, the Cu:Mn molar ratio was fixed at 0.11:0.89 and the sodium acetate content varied within a narrow range. After complete addition, the pH was adjusted to about 9 using ammonium hydroxide, and the solution was heated to 80 °C, under a stream of dry air to evaporate water. The resultant transparent blue gels were decomposed at 500 °C for 10 hours, and then heated to 800 °C for four hours. Solid-state synthesis was carried out by heating a mixture of sodium permanganate, manganese carbonate, and cupric oxide in the molar ratio 5:3:1 to 850° C in air for 18 h. The multiphase product was reground and reheated, after which it was primarily the desired Cu-substituted sodium manganese oxide, with a small amount of residual CuO. An attempt to improve the purity and crystallinity by heating to 950° C produced a single-phase sample with a layered structure similar to that of $Na_{0.7}MnO_2$,[7] but with a larger unit cell. Heat treatment of mixtures containing higher levels of copper did not result in further incorporation of copper into the sodium manganese oxide phase. Ion exchange was carried out by a molten salt procedure described previously.[3] All materials, including the sodium-containing precursors and the ion-exchanged products were characterized by x-ray powder diffraction using a Siemens D5000 diffractometer and Cu Kα radiation.

Whole-pattern structure refinements were carried out using the program RIQAS (Materials Data, Inc.).

Lithium/PEO_8LiTFSI cells were assembled as previously described[6] (PEO is poly(ethylene oxide) and LiTFSI is $LiN(CF_3SO_2)_2$). Cells were equilibrated at 85 °C for at least one hour before testing. A MacPile II (Bio-Logic, SA, Claix, France) potentiostat/galvanostat and an Arbin cycler with ABTS 4.0 software were used for the electrochemical experiments.

Results and Discussion

In the Na-Mn-O system, either layered or tunnel-containing compounds can form during synthesis, depending upon reaction conditions and Na/Mn ratios.[7] The tunnel structure (Fig. 1) is formed above 750 °C in air or oxygen when the Na/Mn ratio is approximately 0.44, the exact ratio varying slightly with the atmosphere and temperature. The structure is complex, with five different Mn sites, for a total of 18 Mn atoms per unit cell. If the Na/Mn ratio is too low, Mn_2O_3 is present as an impurity. If it is too high, a two phase mixture of $Na_{0.44}MnO_2$ and a layered compound with the approximate composition $Na_{0.7}MnO_{2+y}$ results. In the quaternary Na-Mn-Cu-O system, a tunnel compound, in which 11% of the Mn is substituted with Cu, can be synthesized. Even when the Na to transition metal ratio is adjusted to prevent formation of Mn_2O_3 or layered phases, a $CuMn_2O_4$ spinel impurity is sometimes present in reaction products, particularly for those made by sol-gel or GNP when the combustion temperature is high (e.g., the glycine: nitrate ratio is about 0.5:1). Decreasing the glycine: nitrate ratio to 0.33:1 lowers the combustion temperature and reduces the amount of spinel impurity formed. The best results were obtained when a glycine:nitrate ratio of 0.33:1 and a Na:Mn:Cu ratio of

0.41:0.89:0.11 was used for GNP and a Na:Mn:Cu ratio of 0.36:0.89:0.11 was used for sol-gel synthesis. Attempts to synthesize a tunnel compound with a Cu: Mn ratio of 22:78 were unsuccessful, resulting in a mixture of phases. A Cu substitution level of 22-atom % requires the remaining Mn to have an average oxidation state very close to +4, which may be difficult to achieve.

X-ray powder diffraction patterns of the product of the 11% Cu-substituted compound prepared by the glycine-nitrate method and its ion-exchanged lithium-containing analog are shown in Figure 2. The pattern of the sodium-containing precursor resembles that of $Na_{0.44}MnO_2$, but the unit cell volume is slightly smaller (Table I). This decrease is primarily due to the shorter unit cell length in the b direction. Despite its larger size, aliovalent substitution of Cu^{2+} (ionic radius 0.72 Å) for Mn^{4+} (ionic radius 0.60 Å) makes the unit cell smaller because of the corresponding decrease in the amount of Mn^{3+} (ionic radius 0.66 Å).[8] Rietveld refinement of the pattern also gave longer average M-O bond distances and a slightly higher occupancy factor for the Mn3 site. This suggests that Cu substitutes primarily for Mn in Mn3 (half of the Mn3 if only in this site), probably because it is the least constrained of the Mn sites. The refined occupancies at Na1, Na2, and Na3 are 75%, 53%, and 74%, respectively, giving an approximate composition of $Na_{0.45}Cu_{0.11}Mn_{0.89}O_2$ for this product.

Heating this material in a mixture of molten $LiNO_3$ and KNO_3 yields $Li_{0.45-x}Cu_{0.11}Mn_{0.89}O_2$, which is isostructural with the precursor, but has a smaller unit cell. Again, most of the shrinkage is in the b-direction. The smaller unit cell is due both to replacement of the larger sodium ions by Li ions and to slight oxidative

deintercalation during ion exchange. The exact lithium content of this sample was not determined.

Lithium cells with $Li_xCu_{0.11}Mn_{0.89}O_2$ electrodes have an open circuit potential of about 3.3 V, and may either be discharged or charged initially. Figure 3 shows a cyclic voltammogram obtained on an initially charged Li/$P(EO)_8$LITFSI/$Li_xCu_{0.11}Mn_{0.89}O_2$ cell at 85 ºC. Redox processes between 3.6 and 2.5 V appear to be highly reversible, and peaks are seen at about 2.9, 3.1, and 3.3 V. Compared to unsubstituted Li_xMnO_2 with the $Na_{0.44}MnO_2$ structure, some of the capacity is shifted to lower potentials (no features are observed at 2.9 V in differential capacity plots for unsubstituted fully exchanged materials). Interestingly, in cells containing $Li_xTi_yMn_{1-y}O_2$ compounds (where y=0.11, 0.22, 0.33, 0.44 and 0.55) with the $Na_{0.44}MnO_2$ structure, capacity at 2.9 V increases with increasing Ti-content.[9] It appears that this feature may be associated with substitution at the Mn3 site, although the complexities of the Ti distribution patterns in $Li_xTi_yMn_{1-y}O_2$ structures preclude a definitive assignment at this time.

Figure 4 shows a discharge profile at 0.05 mA/cm^2 of a Li/$P(EO)_8$LiTFSI/$Li_xCu_{0.11}Mn_{0.89}O_2$ cell heated to 85 ºC and initially charged to 3.6 V. The profile is gradually sloping and a capacity of about 85 mAh/g is obtained between 3.6 and 2.5V, consistent with the CV results. In contrast, Li_xMnO_2 with the $Na_{0.44}MnO_2$ structure usually delivers about 100 mAh/g in a polymer cell configuration between these voltage limits. Reversible intercalation into materials with the $Na_{0.44}MnO_2$ structure is limited by the number of sites for alkali metal ions rather than by the number of redox centers. A change in composition of $\Delta x = 0.66$ in Li_xMnO_2 (corresponding to about 200 mAh/g) is the maximum reversible theoretical capacity assuming similar site limitations

as for $Na_{0.44}MnO_2$. Thus, it is possible to substitute inactive ions for some of the manganese without adversely impacting the theoretical capacity, because not all of the manganese undergoes redox. For example, in the case of $Li_xTi_yMn_{1-y}O_2$ compounds, the capacity delivered between 3.6 and 2.5V actually increases for y=0.22. It has been suggested[9] that the improvement is due to the larger unit cell size of the 22% Ti substituted material, which allows extraction of more lithium ions from the structure at moderate voltages. The overall effect is to flatten the entire voltage profile somewhat. Further increasing the amount of substitution does not improve capacity, however, and for $Li_xTi_{0.55}Mn_{0.45}O_2$ there is a substantial decrease, suggesting that inactive Ti replaces some normally electro-active Mn at these higher levels.

In Li_xMnO_2, Mn ions in Mn3 sites do not change oxidation state between x=0.27 and 0.62; [10] thus, replacement of half of these ions with Cu in $Li_xCu_{0.11}Mn_{0.89}O_2$ is not expected to reduce the electrochemical capacity between 2.5 and 3.6 V vs. Li. The approximately 15% reduction in utilization upon 11 atom % substitution is more likely due to the contraction in the unit cell volume, which makes it more difficult to extract lithium ions at moderate voltages, steepening the profile. However, the possibility that the order or identity of the Mn ions that undergo redox is changed in substituted tunnel compounds cannot be definitively ruled out at this time.

Conclusions

$Li_xCu_{0.11}Mn_{0.89}O_2$ was prepared and tested as a cathode material for lithium rechargeable batteries. Replacement of 11-atom % of the Mn by Cu caused profound changes in the electrochemical properties; the voltage profile became steeper, causing an effective 15% loss in utilization between 3.6 and 2.5 V vs. Li. Cu-substitution also causes

a decrease in the unit cell size, which appears to be correlated with lower utilization in materials with the $Na_{0.44}MnO_2$ structure. These observations suggest that substitutions that increase unit cell size without unduly decreasing the number of electro-active sites may result in cathodes with higher effective capacities.

Acknowledgment

This work was supported by the Assistant Secretary for Energy Efficiency and Renewable Energy, Office of Transportation Technologies, Office of Advanced Automotive Technologies of the U.S. Department of Energy under Contract No. DE-AC03-76SF00098.

References

1. M. M. Doeff, M. Y. Peng, Y. Ma, and L.C. De Jonghe, *J. Electrochem. Soc.*, **141**, L145 (1994).

2. M. M. Doeff, T. J. Richardson, and L. Kepley, *J. Electrochem. Soc.*, **143**, 2507 (1996).

3. M. M. Doeff, A. Anapolsky, L. Edman, T.J. Richardson, and L. C. De Jonghe, *J. Electrochem. Soc.*, **148**, A230 (2001).

4. M. M. Doeff, K.-T. Hwang, A. Anapolsky, and T. J. Richardson, *Proc. Electrochem. Soc.*, **99-24**, 48 (2000).

5. L.A. Chick, L.R. Pederson, G. D. Maupin, J. L. Bates, L.E. Thomas, and G.J. Exarhos, *Mat. Let.*, **10**, 6 (1990).

6. M. M. Doeff, M. Y. Peng, Y. Ma, and L.C. De Jonghe, *J. Electrochem. Soc.*, **141**, L145 (1994).

7. J.-P. Parant, R. Olazcuaga, M. Devalette, C. Fouassier, and P. Hagenmuller, *J. Solid. State Chem.*, **3**, 1 (1971).

8. *Handbook of Chemistry and Physics*, R. C. Weast, Editor, 68th ed., CRC Press, Inc., Boca Raton, FL (1987-1988).

9. M. M. Doeff, T. J. Richardson, K.-T. Hwang, and L. C. De Jonghe, *J. Electrochem. Soc.*, manuscript in preparation.

10. T. J. Richardson, P. N. Ross, Jr., and M. M. Doeff, *Proc. Electrochem. Soc.,* 98-16, 229 (1999).

Table I. Cell parameters

		a_0 (Å)	b_0 (Å)	c_0 (Å)	Vol. (Å^3)
$Na_{0.44}MnO_2$[a]	solid-state synthesis	9.084	26.479	2.825	679.5
$Na_{0.5}Cu_{0.11}Mn_{0.89}O_2$	solid-state synthesis	9.111	26.234	2.834	677.4
$Na_{0.45}Cu_{0.11}Mn_{0.89}O_2$	GNP	9.087	26.121	2.828	671.3
$Li_{0.45-x}Cu_{0.11}Mn_{0.89}O_2$	GNP, ion exchange	8.906	24.184	2.827	608.9

[a] data from Ref. 2.

Figure Captions

Figure 1. The structure of $Na_{0.44}MnO_2$, looking down the c-axis.

Figure 2. X-ray powder diffraction patterns of (a) $Na_{0.45}Cu_{0.11}Mn_{0.89}O_2$ made by glycine-nitrate combustion and (b) the ion-exchanged product, $Li_{0.45-x}Cu_{0.11}Mn_{0.89}O_2$.

Figure 3. Cyclic voltammogram of a Li/P(EO)$_8$LiTFSI/$Li_xCu_{0.11}Mn_{0.89}O_2$ cell at 85 ºC; scan rate 0.1 mV/sec.

Figure 4. Discharge profile of a Li/P(EO)$_8$LiTFSI/$Li_xCu_{0.11}Mn_{0.89}O_2$ cell at 85 ºC, current density 0.05 mA/cm^2. Cell was initially charged to 3.6 V and rested for one hour prior to discharge.

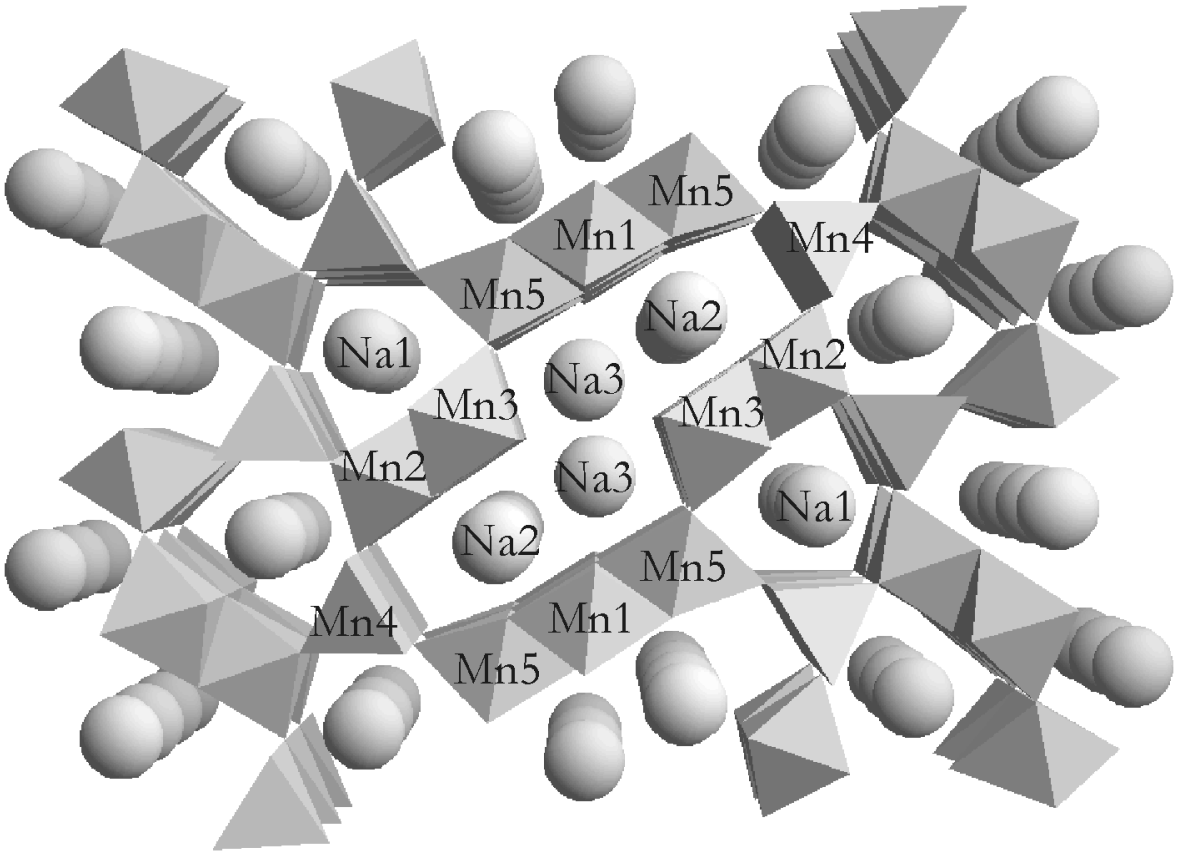

Doeff et al., Figure 1

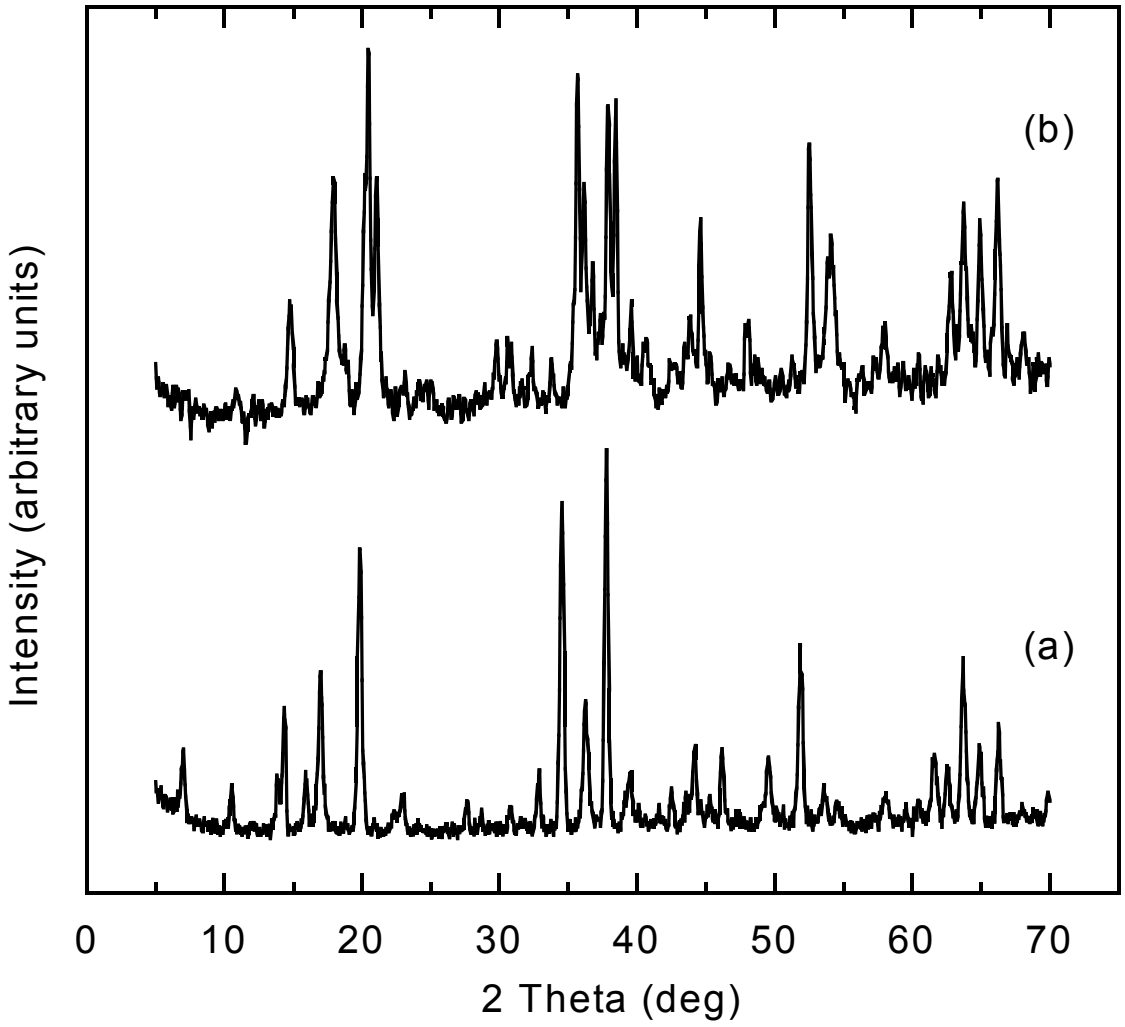

Doeff et al., Figure 2

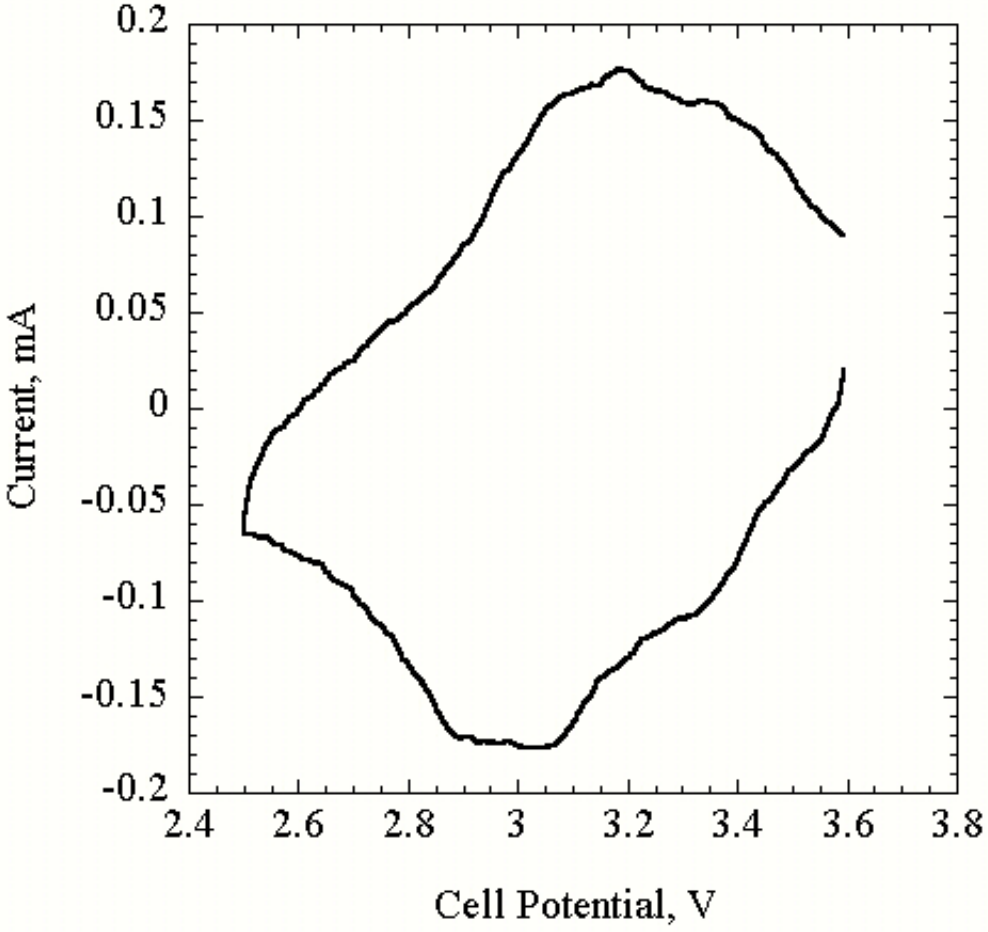

Doeff et al., Figure 3.

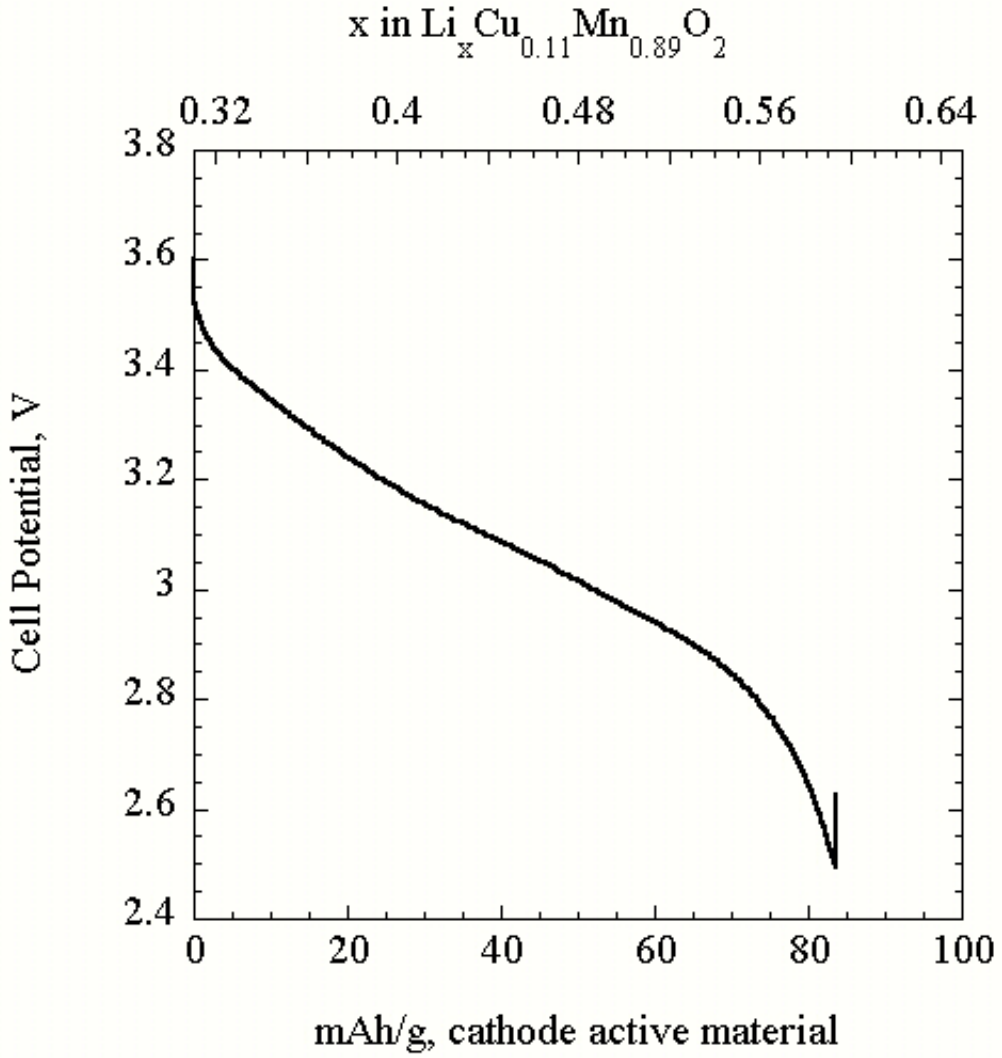

Doeff et al., Figure 4.